Science & Technology Development Journal 2022, 25(3):2460-2468

Open Access Full Text Article

Research article

Decay of charged leptons $l_i \to l_j\gamma$ in the 3-3-1 model with neutral leptons

Ha Thanh Hung*, Vuong Minh Nguyen, Huan Phuc Hoang

ABSTRACT

The 3-3-1 model with neutral leptons exists as a source of lepton-flavor-violating (LFV) due to oscillations of active neutrinos and the mixing of exotic leptons. The investigation of component contributions for $l_i \to l_j\gamma$ helps to select the parameter space regions that are suitable for the current experimental data. We show that in the parameter space regions where $Br(\mu \to e\gamma)$ satisfies the experimental limits, $Br(\tau \to e\gamma)$ and $Br(\tau \to \mu\gamma)$ are also smaller than the upper bound of the experimental data.

Key words: Extensions of electroweak Higgs sector, Electroweak radiative corrections, Neutrino mass, and mixing, etc...

INTRODUCTION

The experimental data on neutrinos confirmed the masses and oscillations of neutrinos [1,2], leading to the appearance of models beyond the standard model (BSM). LFV sources follow BSM as a necessity. This is a favorable condition to study the decay of charged leptons. Accordingly, the strict experimental limits of $l_i \to l_j\gamma$ decays are also given [1,2].

$$\begin{aligned} Br(\mu \to e\gamma) &\le 4.2 \times 10^{-13}, \\ Br(\tau \to e\gamma) &\le 3.3 \times 10^{-8}, \\ Br(\tau \to \mu\gamma) &\le 4.4 \times 10^{-8}. \end{aligned} \quad (1)$$

Theoretically, $l_i \to l_j\gamma$ will appear at one-loop order and increase accuracy when considered at higher loop order. These decays do not exist at the tree level. A previous publication also mentioned the accuracy of $l_i \to l_j\gamma$ [3]. However, due to the existence of very small contributing components, the approximation is more widely used [4,5].

Each LFV decay of charged lepton is satisfied in different regions of the parameter space when considered in a particular model. Therefore, it is of great interest to show the parameter space regions where all decays of charged leptons are satisfied [6–8]. Among the $l_i \to l_j\gamma$ decays, $Br(\mu \to e\gamma)$ has the strictest experimental limit. Thus, in the usual way when $Br(\mu \to e\gamma)$ satisfies the experimental limits, $Br(\tau \to e\gamma)$ and $Br(\tau \to \mu\gamma)$ are also satisfied [6,8]. Recently, $\mu \to e\gamma$ decay has been studied in the 331 model with neutral leptons [9]. In that publication, the parameter space regions satisfying $Br(\mu \to e\gamma)$ are given to predict the large signal of $Br\left(h_0^1 \to \mu\tau\right)$. However, $\tau \to e\gamma$ and $\tau \to \mu\gamma$ have not been studied in detail. For example, what are the main contributors to $Br(\tau \to e\gamma)$ and $Br(\tau \to \mu\gamma)$? What values can $Br(\tau \to e\gamma)$ and $Br(\tau \to \mu\gamma)$ achieve in the parameter regions where $Br(\tau \to e\gamma)$ satisfies the experimental limit?... are all unanswered.

In this work, we study $l_i \to l_j\gamma$ in the 331 model with neutral leptons and solve the above problems. In particular, the parameter space regions are selected to be suitable for the hypothesis related to the active energy 13 TeV of the *Large Hadron Collider (LHC@13TeV)*, where all decays of charged leptons satisfy the experimental limits. We also show the values that lalb can be obtained within those allowed spatial regions.

The paper is organized as follows. In the next section, we review the model, give mass spectra of gauge and Higgs bosons and show the LFV couplings. We use the Feynman rules to give analytic formulas for LFV decays of changed leptons in Section III. Numerical results are discussed in Section IV. The conclusions are presented in Section V.

BRIEF REVIEW OF THE MODEL

The 3-3-1 model with neutral leptons is a specific class of model 331β with parameter $\beta = -\frac{1}{\sqrt{3}}$, which is a successful extension of the standard model (SM) [9,10]. The gauge group of this model is $SU(3)_c \otimes SU(3)_L \otimes U(1)_X$ corresponding to the electric charge operator $Q = T_3 - \frac{1}{\sqrt{3}}T_8 + X$, where $T_{3,8}$ are diagonal $SU(3)_L$ generators and X is the new charge of the group $U(1)_X$. Fermions, including leptons and quarks, are

Department of Physics, Hanoi Pedagogical University 2, Phuc Yen, Vinh Phuc, Vietnam

Correspondence

Ha Thanh Hung, Department of Physics, Hanoi Pedagogical University 2, Phuc Yen, Vinh Phuc, Vietnam

Email: hathanhhung@hpu2.edu.vn

History

- Received: 2022-05-21
- Accepted: 2022-08-03
- Published: 2022-08-31

DOI : 10.32508/stdj.v25i3.3943

VNUHCM PRESS
25 years of scholarly publishing
1997-2022

Cite this article : Hung H T, Nguyen V M, Hoang H P. **Decay of charged leptons $l_i \to l_j\gamma$ in the 3-3-1 model with neutral leptons**. *Sci. Tech. Dev. J.;* 25(3):2460-2468.

assigned as follows:

$$\psi'_{aL} = \begin{pmatrix} \nu'_a \\ e'_a \\ N'_a \end{pmatrix}_L \square \left(1,3,-\frac{1}{3}\right), \quad (2)$$
$$e'_{aR} \square (1,1,-1),\ N'_a \square (1,1,0),$$

where $a = 1,2,3$ are generation indexes and N'_{aR} is the part that differentiates this model from models with right-handed neutrinos. Note that we use commas for the initial states. The first two generations of quarks are classified into antitriplets of the $SU(3)_L$ group, while the other generation is a triplet.

$$Q'_{iL} = \begin{pmatrix} d'_i \\ -u'_i \\ D'_i \end{pmatrix}_L \square \left(3,\bar{3},3\right),$$
$$u'_{iR} \square \left(3,1,\tfrac{2}{3}\right),\ d'_{iR} \square \left(3,1,-\tfrac{1}{3}\right),\ D'_{iR} \square \left(3,1,-\tfrac{1}{3}\right),$$
$$Q'_{3L} = \begin{pmatrix} u'_3 \\ d'_3 \\ U'_3 \end{pmatrix}_L \square \left(3,3,\tfrac{1}{3}\right), \quad (3)$$
$$u'_{3R} \square \left(3,1,\tfrac{2}{3}\right),\ d'_{3R} \square \left(3,1,-\tfrac{1}{3}\right),\ U'_{iR} \square \left(3,1,\tfrac{2}{3}\right),$$

above, we use indexes $i = 1,2$ and $a = 1,2,3$.

To generate masses for the particles, this model needs to include three scalar triplets. where the two triplets η and χ have the same quantum numbers.

$$\eta = \begin{pmatrix} \eta^0 \\ \eta^- \\ \eta'^0 \end{pmatrix} \square \left(1,3,-\frac{1}{3}\right),$$
$$\rho = \begin{pmatrix} \rho^+ \\ \rho^0 \\ \rho'^+ \end{pmatrix} \square \left(1,3,\frac{2}{3}\right), \quad (4)$$
$$\chi = \begin{pmatrix} \chi'^0 \\ \chi^- \\ \chi^0 \end{pmatrix} \square \left(1,3,-\frac{1}{3}\right),$$

The vacuum expectation value (VEV) structure of the neutral components is introduced

$$\eta'^0 = \tfrac{S'_2+iA'_2}{\sqrt{2}},\ \chi'^0 = \tfrac{S'_3+iA'_3}{\sqrt{2}},$$
$$\rho^0 = \tfrac{1}{\sqrt{2}}(v_1+S_1+iA_1),\ \eta^0 = \tfrac{1}{\sqrt{2}}(v_2+S_2+iA_2),$$
$$\chi^0 = \tfrac{1}{\sqrt{2}}(v_3+S_3+iA_3), \quad (5)$$

With the above selection of VEVs, the particles in the model mainly receive their mass at the tree level, with the exception of active neutrinos that gain masses through the effective interaction, η'^0 and χ'^0 were chosen with VEV zero to avoid the occurrence of neutral currents that have a large violation of the total lepton number, as indicated in references[6,11].

The Higgs potential is given in its most common form. Here, only the terms that preserve the lepton number are kept, and the rest are ignored because there are very small accompanying coefficients[10].

$$\begin{aligned} V(\eta,\rho,\chi) &= \mu_1^2\eta^2 + \mu_2^2\rho^2 + \mu_3^2\chi^2 + \lambda_1\eta^4 + \lambda_2\rho^4 \\ &+\lambda_3\chi^4 + \lambda_{12}(\eta^+\eta)(\rho^+\rho) + \lambda_{13}(\eta^+\eta)(\chi^+\chi) \\ &+\lambda_{23}(\rho^+\rho)(\chi^+\chi) + \bar{\lambda}_{12}(\eta^+\rho)(\rho^+\eta) \\ &+\bar{\lambda}_{13}(\eta^+\chi)(\chi^+\eta) + \bar{\lambda}_{23}(\rho^+\chi)(\chi^+\rho) \\ &+\sqrt{2}fv_3(\in^{ijk}\eta_i\rho_j\chi_k + H.c). \end{aligned} \quad (6)$$

The equations for the minimum condition of the Higgs potential are:

$$\begin{aligned} \mu_1^2 &= \frac{fv_1v_3^2}{v_2} - \frac{\lambda_{12}v_1^2+\lambda_{13}v_3^2}{2} - \lambda_1v_2^2, \\ \mu_2^2 &= \frac{fv_2v_3^2}{v_1} - \frac{\lambda_{12}v_2^2+\lambda_{23}v_3^2}{2} - \lambda_2v_1^2, \\ \mu_3^2 &= fv_2v_1 - \lambda_3v_3^2 - \frac{(\lambda_{23}v_1^2+\lambda_{13}v_2^2)}{2}. \end{aligned} \quad (7)$$

We obtain two charged Higgs bosons whose masses and physical states are:

$$\begin{aligned} m_{H_1\pm}^2 &= v_1^2\left(\frac{1}{t_{12}^2}+1\right)\left(\frac{\widetilde{\lambda_{12}}}{2}+\frac{ft_{12}}{t_{13}^2}\right); \\ m_{H_2\pm}^2 &= v_1^2\left(\frac{1}{t_{13}^2}+1\right)\left(\frac{\widetilde{\lambda_{23}}}{2}+\frac{f}{t_{12}}\right), \end{aligned} \quad (8)$$

$$\begin{aligned} \begin{pmatrix} \rho^\pm \\ \eta^\pm \end{pmatrix} &= \begin{pmatrix} -c_{12} & s_{12} \\ s_{12} & c_{12} \end{pmatrix}\begin{pmatrix} G_W^\pm \\ H_1^\pm \end{pmatrix}, \\ \begin{pmatrix} \rho'^\pm \\ \chi^\pm \end{pmatrix} &= \begin{pmatrix} -s_{13} & c_{13} \\ c_{13} & s_{13} \end{pmatrix}\begin{pmatrix} G_V^\pm \\ H_2^\pm \end{pmatrix}. \end{aligned} \quad (9)$$

From the structure of the neutral components, this model will have 4 CP-even neutral Higgs bosons. Therefore, a neutral Higgs boson h_4^0 was combined with a Goldstone boson G_U (corresponding to U-boson).

$$\begin{aligned} \begin{pmatrix} S'_2 \\ S'_3 \end{pmatrix} &= \begin{pmatrix} -s_{13} & c_{13} \\ c_{13} & s_{13} \end{pmatrix}\begin{pmatrix} G_U \\ h_4^0 \end{pmatrix}, \\ m_{h_4^0}^2 &= (v_1^2+v_3^2)\left(\frac{\widetilde{\lambda}_{13}}{2}+\frac{fv_2}{v_1}\right). \end{aligned} \quad (10)$$

In Eqs.(9,10), we use denotations: $s_{ij} = \sin\beta_{ij}$, $c_{ij} = \cos\beta_{ij}$ and $t_{12} = \tan\beta_{12} = \frac{v_2}{v_1}$, $t_{13} = \tan\beta_{13} = \frac{v_1}{v_3}$, $t_{23} = \tan\beta_{23} = \frac{v_2}{v_3}$.

Mass matrix of the remaining 3 neutral Higgs bosons.

$$M_h^2 = \quad (11)$$
$$\begin{pmatrix} 2\lambda_2v_1^2+\frac{fv_2v_3^2}{v_1} & v_1v_2\lambda_{12}-fv_3^2 & v_3(v_1\lambda_{23}-fv_2) \\ v_1v_2\lambda_{12}-fv_3^2 & 2\lambda_1v_2^2+\frac{fv_1v_3^2}{v_2} & v_3(v_2\lambda_{13}-fv_1) \\ v_3(v_1\lambda_{23}-fv_2) & v_3(v_2\lambda_{13}-fv_1) & 2\lambda_3v_3^2+fv_1v_2 \end{pmatrix}$$

We include the relationship between the interaction coefficients as the imposed condition for the masses of the neutral Higgs bosons. This imposed condition has

also been introduced in previous publications such as Refs. [11,12]

$$f = \lambda_{13} t_{12} = \frac{\lambda_{23}}{t_{12}} \tag{12}$$

Based on Eq. (12), the mass matrix now becomes

$$\begin{pmatrix} 2\lambda_2 v_1^2 + \lambda_{13} v_3^2 t_{12}^2 & \left(\lambda_{12} v_1^2 - \lambda_{13} v_3^2\right) t_{12} & 0 \\ \left(\lambda_{12} v_1^2 - \lambda_{13} v_3^2\right) t_{12} & 2\lambda_1 v_2^2 + \lambda_{13} v_3^2 & 0 \\ 0 & 0 & 2\lambda_3 v_3^2 + \lambda_{13} v_2^2 \end{pmatrix} \tag{13}$$

Conspicuously, a heavily neutral Higgs boson has mass $m_{h_3^0}^2 = 2\lambda_3 v_3^2 + \lambda_{13} v_2^2$ (proportional to the energy scale to break the symmetry of the $SU(3)_L \otimes U(1)_X$ group). The remaining two neutral Higgs bosons have masses given by the following technique [11,12], where h_1^0 is the lightest and is identical to the Higgs boson of the standard model (SM-like Higgs boson).

$$\begin{aligned} m_{h_1^0}^2 &= M_{11}^2 \cos^2\delta + M_{22}^2 \sin^2\delta - M_{12}^2 \sin 2\delta, \\ m_{h_2^0}^2 &= M_{11}^2 \sin^2\delta + M_{22}^2 \cos^2\delta - M_{12}^2 \sin 2\delta, \\ M_{11}^2 &= 2\left(s_{12}^4 \lambda_1 + c_{12}^4 \lambda_2 + s_{12}^2 c_{12}^2 \lambda_{12}\right) v^2 = O\left(v^2\right), \\ M_{12}^2 &= \left[-\lambda_1 s_{12}^2 + \lambda_2 c_{12}^2 + \lambda_{12}(s_{12}^2 - c_{12}^2)\right] s_{12} c_{12} v^2 \\ &\quad = O\left(v^2\right), \\ M_{22}^2 &= 2 s_{12} c_{12} \left[\lambda_1 + \lambda_2 - \lambda_{12}\right] v^2 + \frac{\lambda_{13} v_3^2}{c_{12}^2}, \end{aligned} \tag{14}$$

where $\tan 2\delta = \frac{2M_{12}^2}{M_{22}^2 - M_{11}^2} \square O\left(\frac{v^2}{v_3^2}\right)$ and $v^2 = v_1^2 + v_2^2$ (15)

Relationship between the physical state and the original basic

$$\begin{pmatrix} S_1 \\ S_2 \end{pmatrix} = \begin{pmatrix} -s_\alpha & c_\alpha \\ c_\alpha & s_\alpha \end{pmatrix} \begin{pmatrix} h_1^0 \\ h_2^0 \end{pmatrix} \quad and\ \alpha = \beta_{12} - \frac{\pi}{2} + \delta \tag{16}$$

We obtain that the states of neutral Higgs bosons depend on the mixing angle δ, which is a characteristic parameter for THDM. As mentioned in Ref. [13], this parameter constraints $c_\delta > 0.99$ for all THDMs, resulting in $_\delta| \leq 0.14$.

The gauge bosons in the model are given based on the covariance derivative

$$D_\mu = \partial_\mu - i g_3 W_\mu^\alpha T^\alpha - g_1 T^9 X X_\mu, \tag{17}$$

where i is the complex number and T^α, $\alpha = \overline{1,8}$ are the generators of the $SU(3)_L$ group, $T^9 = \frac{1}{\sqrt{6}}$.

Neutral gauge bosons not involved in LFV interactions should be ignored. The charged part is

$$W_\mu^\alpha T^\alpha = \frac{1}{\sqrt{2}} \begin{pmatrix} 0 & W_\mu^+ & U_\mu^0 \\ W_\mu^- & 0 & V_\mu^- \\ U_\mu^{0*} & V_\mu^+ & 0 \end{pmatrix} \tag{18}$$

where $W_\mu^\pm = \frac{W_\mu^1 \pm i W_\mu^2}{\sqrt{2}}$; $V_\mu^\pm = \frac{W_\mu^6 \pm i W_\mu^7}{\sqrt{2}}$; $U_\mu^{0*,0} = \frac{W_\mu^4 \pm i W_\mu^5}{\sqrt{2}}$ and their masses

$$\begin{aligned} m_W^2 &= \frac{g^2}{4}\left(v_1^2 + v_2^2\right), \\ m_U^2 &= \frac{g^2}{4}\left(v_2^2 + v_3^2\right), \\ m_V^2 &= \frac{g^2}{4}\left(v_1^2 + v_3^2\right) \end{aligned} \tag{19}$$

Lagrangian Yukawa for leptons

$$\begin{aligned} -L_{lepton}^{Yukawa} &= h_{ab}^{\in} \bar{Y}_a^{'} r e_{bR}^{'} + h_{ab}^N \bar{Y}_a^{'} \chi N_{bR}^{'} \\ &+ \frac{h_{ab}^v}{\Lambda}\left(\overline{\left(Y_a^{'}\right)^c} \eta^*\right)\left(\eta^+ Y_b^{'}\right) + h.c., \end{aligned}$$

Based on scalar triplets, the mass term is given

$$\begin{aligned} &-L_{lepton}^{mass} = \\ &\left[\frac{h_{ab}^{\in} v_1}{\sqrt{2}} \overline{r} e_{aL}^{'} e_{bR}^{'} + \frac{h_{ab}^N v_3}{\sqrt{2}} \overline{N_{aL}^{'}} N_{bR}^{'} + h.c.\right] \\ &+ \frac{h_{ab}^v v_2^2}{2\Lambda}\left[\left(\overline{v_{aR}^{'c}} v_{bL}^{'}\right) + h.c.\right]. \end{aligned} \tag{20}$$

To solve the mixing of leptons, we introduce the U_{ab} and V_{ab} matrices, which are the relationships between the initial and mass bases of active neutrinos and neutral leptons, respectively. We also use comma notation for initial states.

$$\begin{aligned} &e_{aL}^{'-} = e_{aL}^-,\ e_{aR}^{'-} = e_{aR}^-,\ \nu_{aL}^{'} = U_{ab} \nu_{bL}, \\ &N_{aL}^{'} = V_{ab}^L N_{bL},\ N_{aR}^{'} = V_{ab}^R N_{bR}, \end{aligned} \tag{21}$$

The charged leptons are not mixed $m_{e_a} = \frac{v_1}{\sqrt{2}} h_a^e$, $h_a^e = h_{ab}^e \delta_{ab}$, and the masses of active neutrinos and neutral leptons are

$$\begin{aligned} &\frac{v^2}{\Lambda} U^{L+} H^\nu U^L = Diagonal\left(m_{\nu_1}, m_{\nu_2}, m_{\nu_3}\right), \\ &H^\nu = h_{ab}^\nu \\ &\frac{v_3}{\sqrt{2}} V^{L+} H^N V^R = Diagonal\left(m_{N_1}, m_{N_2}, m_{N_3}\right), \\ &H^N = h_{ab}^N \end{aligned} \tag{22}$$

The Yukawa interaction related to the LFV decays of charged leptons in this model is derived from the following Lagrangian term.

$$\begin{aligned} &-L_{lepton}^{Yu} = \frac{m_{e_b}}{v_1}\sqrt{2}[r^0 \overline{e_b} P_R e_b + U_{ba}^* \bar{\nu}_a P_R e_b r^+ \\ &+ V_{ba}^{L*} \overline{N_a} P_R e_b r' + h.c.] + \frac{m_{\nu_a}}{v_2}[S_2 \bar{\nu}_a P_L \nu_b + \\ &\frac{1}{\sqrt{2}} \eta^+\left(U_{ba}^* \bar{\nu}_a P_L e_b + U_{ba} \overline{e_b^c} P_L \nu_a\right) + h.c.] \\ &+ \frac{m_{N_a}}{v_3}\sqrt{2}\left[\chi^0 \overline{N_a} P_R N_a + V_{ba}^{L*} \overline{e_b} P_R N_a \chi^- \_ h.c.\right], \end{aligned} \tag{23}$$

The self-couplings of the Higgs fields are determined from the Higgs potential, and the interactions of the

Higgs and gauge bosons are determined from the kinetic energy terms of the scalar fields. The interactions of the gauge bosons and leptons are determined from the kinetic energy terms of the leptons.

$$L^D_{lepton} = i\overline{L'_a}\gamma^\mu D_\mu L'_a \rightarrow \frac{g}{\sqrt{2}}\left[\begin{array}{l} U^*_{ba}\overline{\nu_a}\gamma^\mu P_L e_b W^+_\mu + U_{ab}\overline{e_c}\gamma^\mu P_L \nu_a W^-_\mu \\ +V^*_{ba}\overline{N_a}\gamma^\mu P_L e_b V^+_\mu + V^L_{ab}\overline{e_b}\gamma^\mu P_L N_a V^-_\mu \end{array}\right] \quad (24)$$

From the above results, we list the couplings as follows:

ANALYTIC FORMULAS FOR $l_i \to l_j\gamma$ DECAYS

From the results in Table 1, we have the Feynman diagrams for $l_i \to l_j\gamma$ decays at one-loop order. The active neutrinos only combine with $W^\pm$-boson and $H_1^\pm$, whereas N_a only combine with $V^\pm$-boson and $H_2^\pm$, so we obtain 4 diagrams as follows.

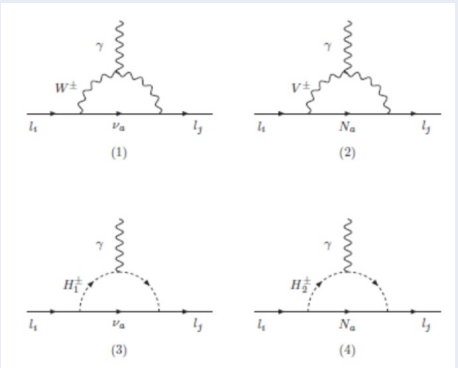

Figure 1: All Feynman diagrams at one-loop order of $l_i \to l_j\gamma$ decays in the 3-3-1 model with neutral leptons

Using the Passarino-Veltman (PV) functions as mentioned in[3,6], with notations: $C_{0,n} = C_{0,n}\left(p_k^2, m_1^2, m_2^2, m_3^2\right)$ and $C_{mn} = C_{mn}\left(p_k^2, m_1^2, m_2^2, m_3^2\right)$, where m; n = 1,2 and $p_k = p_i, p_j$ are the momentum of the charged lepton, and m_1, m_2, m_3 are the masses of the particles in the loop, we have analytic formulas for each diagram.

With diagram (1) in Figure 1,

$$\begin{aligned} D^{\nu_a WW}_{(ij)L}\left(m^2_{\nu_a}, m^2_W\right) &= -\frac{eg^2 m_{e_j}}{32\pi^2}\times \\ &[2\left(C_1 + C_{12} + C_{22}\right) + \frac{m^2_{e_i}}{m^2_W}\left(C_{11} + C_{12} - C_1\right) \\ &+ \frac{m^2_{\nu_a}}{m^2_W}\left(C_0 + C_{12} + C_{22} - C_1 - 2C_2\right)], \\ D^{\nu_a WW}_{(ij)R}\left(m^2_{\nu_a}, m^2_W\right) &= -\frac{eg^2 m_{e_j}}{32\pi^2}\times \\ &[2\left(C_2 + C_{11} + C_{12}\right) + \frac{m^2_{e_j}}{m^2_W}\left(C_{12} + C_{22} - C_2\right) \\ &+ \frac{m^2_{\nu_a}}{m^2_W}\left(C_0 + C_{11} + C_{12} - 2C_1 - C_2\right)], \end{aligned} \quad (25)$$

With diagram (2) in Figure 1,

$$\begin{aligned} D^{N_a WW}_{(ij)L}\left(m^2_{\nu_a}, m^2_W\right) &= -\frac{eg^2 m_{e_j}}{32\pi^2}\times \\ &[2\left(C_1 + C_{12} + C_{22}\right) + \frac{m^2_{e_i}}{m^2_V}\left(C_{11} + C_{12} - C_1\right) \\ &+ \frac{m^2_{N_a}}{m^2_V}\left(C_0 + C_{12} + C_{22} - C_1 - 2C_2\right)], \\ D^{N_a VV}_{(ij)R}\left(m^2_{N_a}, m^2_V\right) &= -\frac{eg^2 m_{e_j}}{32\pi^2}\times \\ &[2\left(C_2 + C_{11} + C_{12}\right) + \frac{m^2_{e_j}}{m^2_V}\left(C_{12} + C_{22} - C_2\right) \\ &+ \frac{m^2_{N_a}}{m^2_V}\left(C_0 + C_{11} + C_{12} - 2C_1 - C_2\right)], \end{aligned} \quad (26)$$

With diagram (3) in Figure 1,

$$\begin{aligned} D^{\nu_a H_1 H_1}_{(ij)L}\left(m^2_{\nu_a}, m^2_{H_1}\right) &= -\frac{eg^2 m_{e_j}}{64\pi^2}\times \\ &[\frac{m^2_{e_i}}{m^2_W}\left(C_{11} + C_{12} - C_1\right) + \frac{m^2_{\nu_a}}{m^2_W}\left(C_{12} + C_{22} - C_2\right) \\ &+ \frac{m^2_{\nu_a}}{m^2_W}\left(C_1 + C_2 - C_0\right)], \\ D^{\nu_a H_1 H_1}_{(ij)R}\left(m^2_{\nu_a}, m^2_{H_1}\right) &= -\frac{eg^2 m_{e_j}}{64\pi^2}\times \\ &[\frac{m^2_{e_i}}{m^2_W}\left(C_{12} + C_{22} - C_2\right) + \frac{m^2_{\nu_a}}{m^2_W}\left(C_{11} + C_{12} - C_1\right) \\ &+ \frac{m^2_{\nu_a}}{m^2_W}\left(C_1 + C_2 - C_0\right)], \end{aligned} \quad (27)$$

With diagram (4) in Figure 1,

$$\begin{aligned} D^{N_a H_2 H_2}_{(ij)L}\left(m^2_{N_a}, m^2_{H_2}\right) &= -\frac{eg^2 m_{e_j}}{32\pi^2}\times \\ &[\frac{m^2_{e_i}}{m^2_V}\left(C_{11} + C_{12} - C_1\right) + \frac{m^2_{N_a}}{m^2_V}\left(C_{12} + C_{22} - C_2\right) \\ &+ \frac{m^2_{N_a}}{m^2_V}\left(C_1 + C_2 - C_0\right)], \\ D^{\nu_a H_2 H_2}_{(ij)R}\left(m^2_{N_a}, m^2_{H_2}\right) &= -\frac{eg^2 m_{e_j}}{32\pi^2}\times \\ &[\frac{m^2_{e_i}}{m^2_V}\left(C_{12} + C_{22} - C_2\right) + \frac{m^2_{N_a}}{m^2_V}\left(C_{11} + C_{12} - C_1\right) \\ &+ \frac{m^2_{N_a}}{m^2_V}\left(C_1 + C_2 - C_0\right)], \end{aligned} \quad (28)$$

Table 1: The couplings are related to $l_i \to l_j\gamma$ decays in the unitary gauge.

Vertex	Coupling	Vertex	Coupling
$\bar{\nu}_a e_b H_1^+$	$-i\sqrt{2}U_{ba}^{L*}\left(\frac{m_{e_b}}{v_1}c_{12}P_R+\frac{m_{\nu_a}}{v_2}s_{12}P_L\right)$	$\bar{e}_b \nu_a H_1^-$	$-i\sqrt{2}U_{ba}^{L}\left(\frac{m_{e_b}}{v_1}c_{12}P_L+\frac{m_{\nu_a}}{v_2}s_{12}P_R\right)$
$\bar{N}_a e_b H_2^+$	$-i\sqrt{2}V_{ba}^{L*}\left(\frac{m_{e_b}}{v_1}c_{13}P_R+\frac{m_{N_a}}{v_3}s_{13}P_L\right)$	$\bar{e}_a N_b H_2^-$	$-i\sqrt{2}V_{ba}^{L}\left(\frac{m_{s_b}}{v_1}c_{13}P_L+\frac{m_{N_a}}{v_3}s_{13}P_R\right)$
$\bar{N}_a e_b V_\mu^+$	$\frac{ig}{\sqrt{2}}V_{ba}^{L*}\gamma^\mu P_L$	$\bar{e}_b N_a V_\mu^-$	$\frac{ig}{\sqrt{2}}V_{ab}^{L}\gamma^\mu P_L$
$\bar{\nu}_a e_b W_\mu^+$	$\frac{ig}{\sqrt{2}}U_{ba}^{L*}\gamma^\mu P_L$	$\bar{e}_b \nu_a W_\mu^-$	$\frac{ig}{\sqrt{2}}U_{ab}^{L}\gamma^\mu P_L$

Based on Ref. [14], the total branching ratios of the $l_i \to l_j\gamma$ processes are

$$Br^{Total}\left(l_i \to l_j\gamma\right) \\ \square \frac{48\pi^2}{G_F^2}\left(\left|{}_{(ij)R}\right|^2+\left|{}_{(ji)L}\right|^2\right)Br\left(l_i \to l_j\bar{\nu}_j\nu_i\right) \quad (29)$$

where $G_F = \frac{g^2}{4\sqrt{2}m_W^2}$, $D_{(ij)L} = \sum_a\left(D_{(ij)L}^{\nu_a WW}+D_{(ji)L}^{\nu_a H_1H_1}+D_{(ij)L}^{N_aVV}+D_{(ji)L}^{N_aH_2H_2}\right)$, $D_{(ij)R} = \sum_a\left(D_{(ij)R}^{\nu_a WW}+D_{(ji)R}^{\nu_a H_1H_1}+D_{(ij)R}^{N_aVV}+D_{(ji)R}^{N_aH_2H_2}\right)$, and for different charge lepton decays, we use experimental data $Br\left(\mu \to e\bar{\nu}_e\nu_u\right) = 100\%$; $Br\left(\tau \to e\bar{\nu}_e\nu_\tau\right) = 17,82\%$; $Br\left(\tau \to \mu\bar{\nu}_\mu\nu_\tau\right) = 17,39\%$.

For ordinary charged leptons, we have $m_i \square m_j$, $(i > j)$, resulting in ${}_{(ij)R}\left|\square\ {}_{(ij)L}\right|$, so we can use an approximation as mentioned in Refs. [3,6]

$$Br^{Total}\left(l_i \to l_j\gamma\right) \\ \square \frac{48\pi^2}{G_F^2}\left(\left|D_{(ij)R}\right|^2\right)Br\left(l_i \to l_j\bar{\nu}_j\nu_i\right) \quad (30)$$

To investigate in detail the components contributing to $l_i \to l_j\gamma$, we set up the analytic parts corresponding to the contributions of active neutrinos, neutral leptons and $W^\pm$-bosons as follows:

$$Br^{\nu}\left(l_i \to l_j\gamma\right)\square\frac{48\pi^2}{G_F^2}\times \\ \left|\sum_a\left(D_{(ij)R}^{\nu_a WW}+D_{(ij)R}^{\nu_a H_1H_1}\right)\right|Br\left(l_i \to l_j\bar{\nu}_j\nu_i\right), \quad (31)$$

$$Br^{N}\left(l_i \to l_j\gamma\right)\square\frac{48\pi^2}{G_F^2}\times \\ \left|\sum_a\left(D_{(ij)R}^{N_a WW}+D_{(ij)R}^{N_a H_2H_2}\right)\right|Br\left(l_i \to l_j\bar{\nu}_j\nu_i\right), \quad (32)$$

$$Br^{\nu W}\left(l_i \to l_j\gamma\right)\square\frac{48\pi^2}{G_F^2}\times \\ \left|\sum_a\left(D_{(ij)R}^{\nu_a WW}\right)\right|Br\left(l_i \to l_j\bar{\nu}_j\nu_i\right). \quad (33)$$

We use Eqs. (31-33) to examine the components that contribute to $l_i \to l_j\gamma$ decays in the next numerical investigation.

NUMERICAL RESULTS

We use the well-known experimental parameters [1,2]: charged lepton mass $m_e = 5.10^{-4}\ GeV$, $m_\mu = 0.105\ GeV$, $m_\tau = 1.776\ GeV$, SM-like Higgs mass $m_{h_1^0} = 125,1\ GeV$, mass of the W boson $m_W = 80.385\ GeV$ and gauge coupling of the $SU(2)_L$ symmetry $g = 0.651$.

To match the results as Refs. [15,16], the mass of the Z'-boson in this model is $m_{Z'} = \frac{g^2v_3^2c_W^2}{3-4s_W^2}$, which must satisfy $m_{Z'} \geq 4.0\ TeV$, resulting in $v_3 \geq 10.1\ TeV$. At LHC@13TeV, we choose $v_3 = 13\ TeV$, resulting in $m_V \geq 4.2\ TeV$. Thus, we fix $m_V = 4.2\ TeV$ in the investigations below.

Based on works [11,17–19], we also choose to fix the following parameters: $t_{12} = 0.5$, $m_{H_1^\pm} = 0.6\ TeV$

Using the results from the experiment [1,2,20], $\triangle m_{21}^2 = 7.55 \times 10^{-5}\ eV^2$, $\triangle m_{31}^2 = 2.424 \times 10^{-3}\ eV^2$, $\sin^2\theta_{12}^v = 0.32$, $\sin^2\theta_{23}^v = 0.547$, and $\sin^2\theta_{13}^v = 0.0216$, we give the oscillation mechanism of active neutrinos according to the U^{PMNS} matrix.

According to Ref. [21], we have a relationship as

$$U^{PMNS} = U_l^+\left(1+\eta\right)U^L \quad (34)$$

where U^L is the unitary matrix mentioned in Eq. (20) and U_l^+ diagonalize the charged lepton mass matrix m_{l_i} with $U_l m_l m_l^+ U_l^+ = diag\left(m_e^2, m_\mu^2, m_\tau^2\right)$. However, we will work in the basis in which the charged lepton mass matrix is diagonal; then, we set $U_l = 1$. The matrix η parametrises the deviation from the unitarity of the neutrino mixing matrix (34); it is very small that one can ignore. Therefore, $U^{PMNS} \approx U^L$, and using the standard parameterized PDG, the U matrix is introduced in the following form [21]:

$$U\left(\theta_{12},\theta_{13},\theta_{23}\right) = \begin{pmatrix}1 & 0 & 0\\ 0 & \cos\theta_{23} & \sin\theta_{23}\\ 0 & -\sin\theta_{23} & \cos\theta_{23}\end{pmatrix} \\ \begin{pmatrix}\cos\theta_{13} & 0 & \sin\theta_{23}\\ 0 & 1 & 0\\ -\sin\theta_{13} & 0 & \cos\theta_{23}\end{pmatrix}\begin{pmatrix}\cos\theta_{12} & \sin\theta_{12} & 0\\ -\sin\theta_{12} & \cos\theta_{12} & 0\\ 0 & 0 & 1\end{pmatrix}. \quad (35)$$

For active neutrinos, we use assignment $U_{ab}^L \equiv U\left(\theta_{12}^v,\theta_{13}^v,\theta_{23}^v\right)$, $U_{ab}^{L+} \equiv U^+\left(\theta_{12}^v,\theta_{13}^v,\theta_{23}^v\right)$, where

$\theta_{12}^{v}, \theta_{13}^{v}, \theta_{23}^{v}$ are the mixing angles of the active neutrinos in three generations and are derived from the experiment.

Exotic leptons are also assumed to be mixed as above with $V_{ab}^{L} \equiv U\left(\theta_{12}^{N}, \theta_{13}^{N}, \theta_{23}^{N}\right)$, where $\theta_{12}^{N}, \theta_{13}^{N}, \theta_{23}^{N}$ are mixing angles of exotic leptons.

In this model, the LFV source comes from a mixture of neutrinos and neutral leptons. In this model, the LFV source comes from a mixture of neutrinos and neutral leptons. The neutrinos are fixed mixed according to the aforementioned experimental data. Therefore, to have a large LFV source, we can choose V_{ab}^{L} in the following cases[21]: i) $V_{ab}^{L} = U\left(\frac{\pi}{4}, \frac{\pi}{4}, \frac{\pi}{4}\right)$, ii) $V_{ab}^{L} = U\left(\frac{\pi}{4}, \frac{\pi}{4}, -\frac{\pi}{4}\right)$, iii) $V_{ab}^{L} = U\left(\frac{\pi}{4}, 0, 0\right)$. However, the study of $l_i \to l_j\gamma$ in these cases was done in the same way[9]. Therefore, we perform the analysis with the specific case of $V_{ab}^{L} = U\left(\frac{\pi}{4}, \frac{\pi}{4}, \frac{\pi}{4}\right)$.

First, we perform a numerical investigation with $\mu \to e\gamma$ decay, which is the decay of the charged lepton with the strictest limit, and the remaining decays will be done in the same way. The components that contribute to $\mu \to e\gamma$ decay are shown in the left panel of Figure 2.

The contributions of W-bosons (Br^{vW}) and active neutrinos (Br^{v}) are very small compared with those of exotic leptons (Br^{N}), so Br^{N} is the main contributor to $Br(\mu \to e\gamma)$. In the right panel of Figure 2, we show that $Br(\mu \to e\gamma)$ decreases as m_V increases, and if $m_V = 4.2\ TeV$ is selected, $Br(\mu \to e\gamma) < 4.2 \times 10^{-13}$ in the domain $m_{H_2^{\pm}} < 5.0\ TeV$. This result suggests that we find parameter space domains satisfying the experimental limit of $\mu \to e\gamma$ decay when $m_V = 4.2\ TeV$ is fixed.

Fixed m_{N_1} or m_{N_2}, we show the regions of the parameter space satisfying the experimental limit of $\mu \to e\gamma$ decay as the left panel or right panel of Figure 3.

The results from Figure 3 show that $Br(\mu \to e\gamma)$ can satisfy the experimental upper bound in the domain $m_{H_2^{\pm}} < 5.0\ TeV$. In this domain, an interesting property appears, while in the left panel, $Br(\mu \to e\gamma)$ decreases with m_{N_1}, while in the right panel, $Br(\mu \to e\gamma)$ increases with m_{N_2}.

The parameter space regions that satisfy the experimental limits of $Br(\mu \to e\gamma)$ are shown in Figure 4. The yellow part is excluded because it crosses the upper bound of $Br(\mu \to e\gamma)$.

Next, we investigate $\tau \to e\gamma$ decay and $\tau \to \mu\gamma$ decay in exactly the same way as above.

We also show that the contributions of exotic leptons are the main contributors to the decay of $\tau \to e\gamma$ and $\tau \to \mu\gamma$ in Figure 5, and when $m_V = 4.2\ TeV$ is fixed, there will be regions of the parameter space satisfying the experimental limit of $l_i \to l_j\gamma$ in Figure 6.

The numerical investigation of all three $l_i \to l_j\gamma$ decays is shown in Figure 7. We represent the black curves as the constant values of $Br(\mu \to e\gamma)$, the blue dashed curves as the constant values of $Br(\tau \to e\gamma)$ and the magenta dashed curves as the constant values of $Br(\tau \to \mu\gamma)$.

From the results in Figure 7, the parameter space regions are selected to satisfy the strictest limit of $Br(\mu \to e\gamma) \leq 4.2 \times 10^{-13}$, which gives signals of $Br(\tau \to e\gamma)$ and $Br(\tau \to \mu\gamma)$ of approximately 10^{-12} and 10^{-13}, respectively. These ranges all satisfy the upper limit of the current experimental data.

CONCLUSIONS

In the 3-3-1 model with neutral leptons, the LFV signal depends strongly on the mixing of exotic leptons. We choose a hypothesized case ($V_{ab}^{L} = U\left(\frac{\pi}{4}, \frac{\pi}{4}, \frac{\pi}{4}\right)$) that can give the large LFV source to study $l_i \to l_j\gamma$ decays.

The contributions of W-bosons and active neutrinos to $Br\left(l_i \to l_j\gamma\right)$ are very small, so the contributions of exotic leptons are considered the main contribution. At LHC@13TeV, we show that the model under consideration exhibits parameter space regions satisfying the experimental limits of $l_i \to l_j\gamma$ decays with $m_v \square 4.2\ TeV$ and $m_{H_2^{\pm}} < 5.0\ TeV$.

We also show that in the regions where $Br(\mu \to e\gamma) \leq 4.2 \times 10^{-13}$, then $Br(\tau \to e\gamma)$ and $Br(\tau \to \mu\gamma)$ satisfy the experimental limits. However, the signals of $Br(\tau \to e\gamma)$ and $Br(\tau \to \mu\gamma)$ are approximately 10^{-12} and 10^{-13}, respectively. Together with the results regarding the contributors shown in Fig. 5, these are new results not still mentioned in Ref.[9]. Obviously, the values that $Br(\tau \to \mu\gamma)$ and $Br(\tau \to \mu\gamma)$ can obtain are still very small compared to the upper limit of the current experimental data. With the LHLHC project, the LFV signals will be experimentally detected at a higher level of accuracy, as mentioned in Ref.[22] then, we can expect the aforementioned signals to be found in accelerators.

ACKNOWLEDGMENT

This research is funded by Vietnam National Foundation for Science and Technology Development (NAFOSTED) under grant number 103.01-2020.01.

CONFLICT OF INTEREST

The authors declare that they have no known competing financial interests or personal relationships that could have appeared to influence the work reported in this paper.

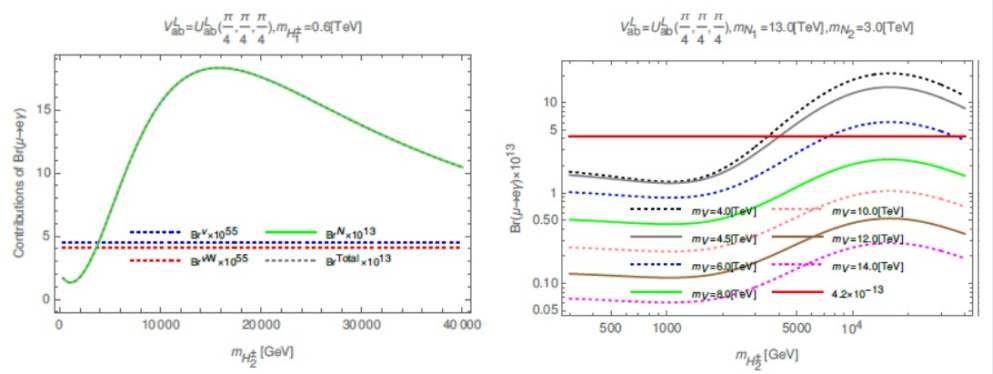

Figure 2: Contributors to $\mu \to e\gamma$ decay depend on $m_{H_2^\pm}$ (left panel) and the dependences of $Br(\mu \to e\gamma)$ on both m_V and $m_{H_2^\pm}$ (right panel).

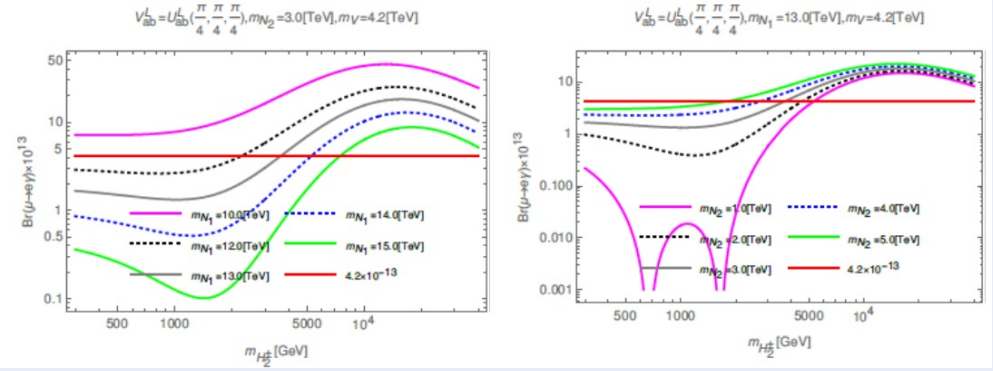

Figure 3: The dependences of $Br(\mu \to e\gamma)$ on m_{N_1} and $m_{H_2^\pm}$ (left panel) or m_{N_2} and $m_{H_2^\pm}$ (right panel)

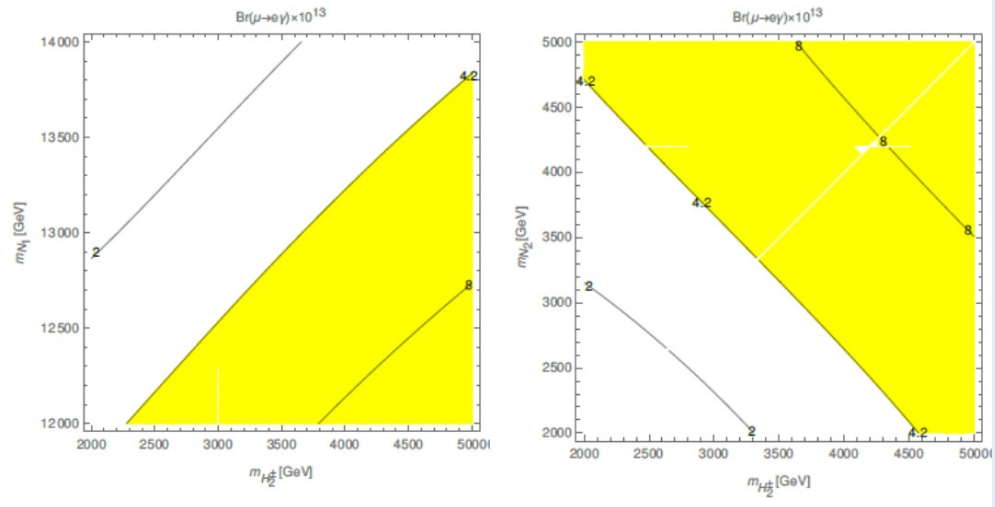

Figure 4: Contour plots of $Br(\mu \to e\gamma)$ depend on m_{N_1} and $m_{H_2^\pm}$ (left panel) or m_{N_2} and $m_{H_2^\pm}$ (right panel)

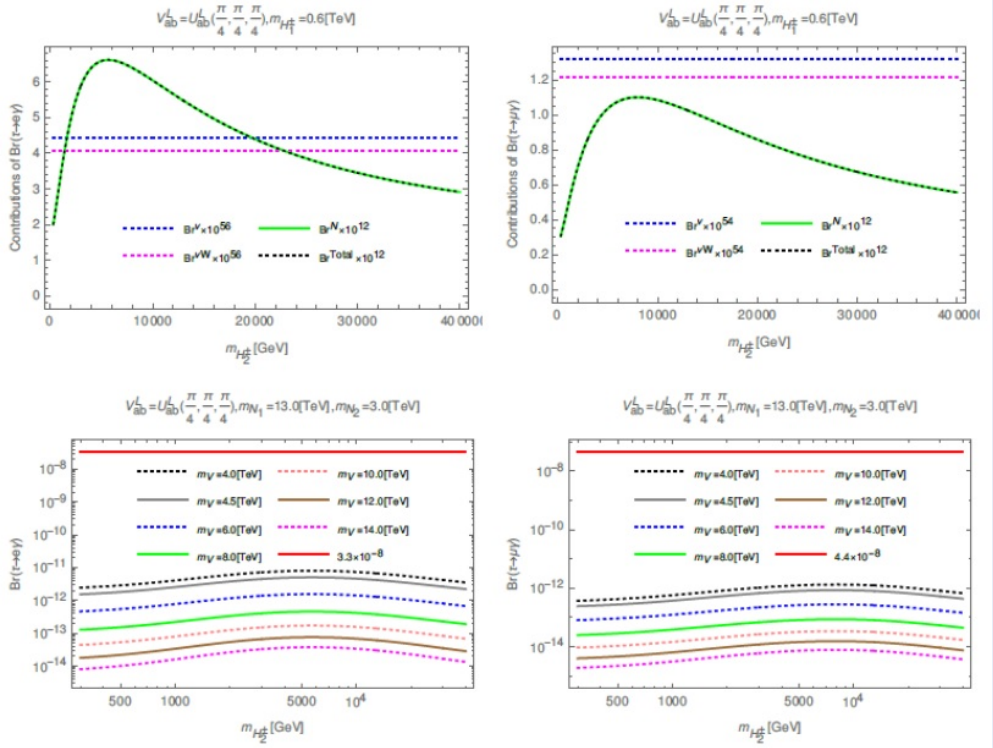

Figure 5: The contributing components (first row) and the influence of m_V (second row) on $\tau \to e\gamma$ (left panel) or $\tau \to \mu\gamma$ (right panel) depend on $m_{H_2^\pm}$.

AUTHOR CONTRIBUTIONS

H. T. Hung: investisgate numerical, discuss and write the contents.

N. M. Vuong: establish analytic formulas for decays of charged lepton.

H. P. Huan: brief review of the model and establish LFV couplings.

REFERENCES

1. Patrignani C et al. (Particle Data Group). Chin Phys C. 2016;40.
2. Particle Data Group, Zyla PA et al. PTEP. 2020;.
3. Hue LT, Ninh LD, Thuc TT, Dat NTT. Eur. Phys. J. C 78, 128 (2018), 1708.09723;.
4. Hue LT, Hung HT, Tham NT, Long HN, Nguyen TP. Phys. Rev. D 104, 033007 (2021), 2104.01840;.
5. Hue LT, Phan KH, Nguyen TP, Long HN, Hung HT. 2109.06089; 2021;.
6. Hung HT, Tham NT, Hieu TT, Hang NTT. PTEP. 2021, 083B01 (2021):2103.16018;.
7. Hong TT, Hung HT, Phuong HH, Phuong LTT, Hue LT. PTEP. 2020, 043B03 (2020), 2002.06826;.
8. Hue LT, et al. Communications in Physics. 2019;29(1):87–96.
9. Hung HT, Binh DT, Quyet HV. (2022), arXiv: 2204.01109;Available from: arXiv:hep-ph/0603098:arXiv:2204.01109.
10. Chang D, Long HN. Phys. Rev. D. 2006;73:053006. Available from: arXiv:hep-ph/0603098.
11. Hung HT, Hong TT, Phuong HH, Mai HLT, Hue LT. Phys. Rev. D 100, 075014 (2019);.
12. Okada H, Okada N, Orikasa Y, Yagyu K. Phys. Rev. D 94, 015002 (2016), 1604.01948;.
13. Kanemura S, Kikuchi M, Mawatari K, Sakurai K, Yagyu K. Phys Lett B. 2018, 1803.01456;783:140;Available from: https://doi.org/10.1016/j.physletb.2018.06.035.
14. Crivellin A, Hoferichter M, Schmidt-Wellenburg P. Phys Rev D. 2018;98, 113002:1807.11484;.
15. CMS, Sirunyan AM et al. J Hepatol. 2018, 1803.06292;06:120;.
16. ATLAS G Aad et al. Phys Lett B. 2019, 1903.06248;796:68;.
17. Cepeda M et al. CERN yellow rep. Monogr. 2019, 1902.00134;7:221;.
18. ATLAS G. Aad et al., Phys. Rev. Lett. 114, 231801 (2015), 1503.04233;PMID: 26196792.
19. CMS, Khachatryan V et al. J Hepatol. 2015, 1508.07774;11:018;.
20. Ibarra A, Molinaro E, Petcov ST. J Hepatol. 2010;09(108):1007.2378;Available from: https://doi.org/10.1007/JHEP09(2010)108.
21. Hue LT, Long HN, Thuc TT, Phong Nguyen TP. Nucl. Phys. B 907, 37 (2016), 1512.03266;.
22. Altmannshofer W, Caillol C, Dam M, Xella S, Zhang Y. Charged lepton flavor violation in heavy particle DEcays, in 2022 Snowmass summer study; 2022. p. 2205.10576;.

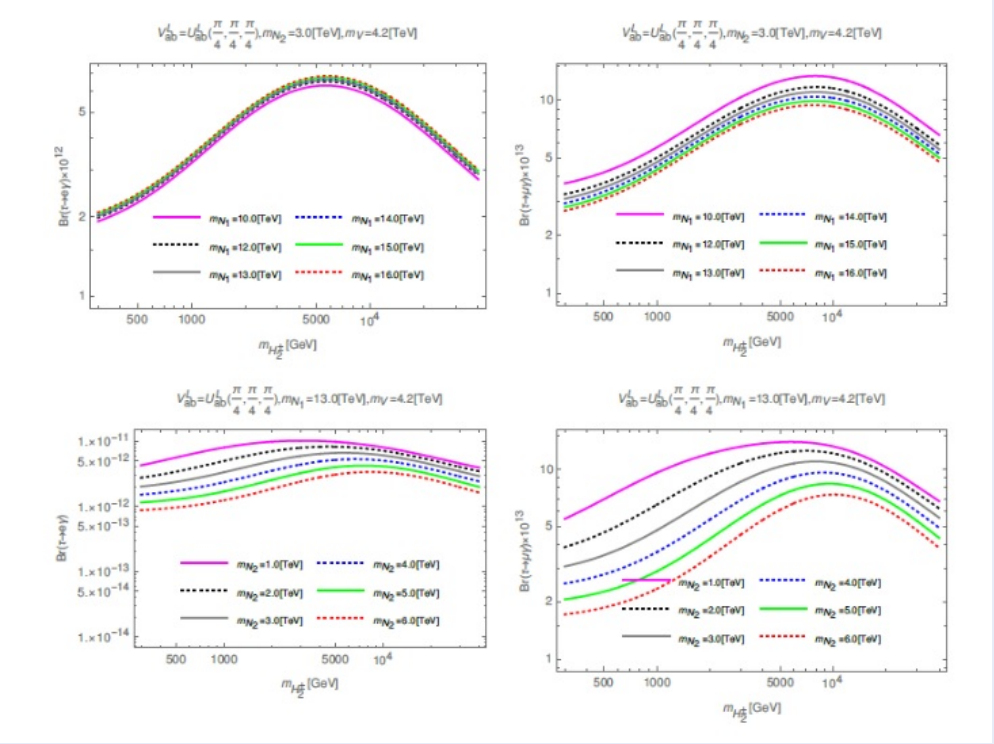

Figure 6: Plots of $Br(\tau \to e\gamma)$ (left panel) or $Br(\tau \to \mu\gamma)$ (right panel) dependon m_{N_1} and $m_{H_2^\pm}$ (first row) or m_{N_2} and $m_{H_2^\pm}$ (second row)

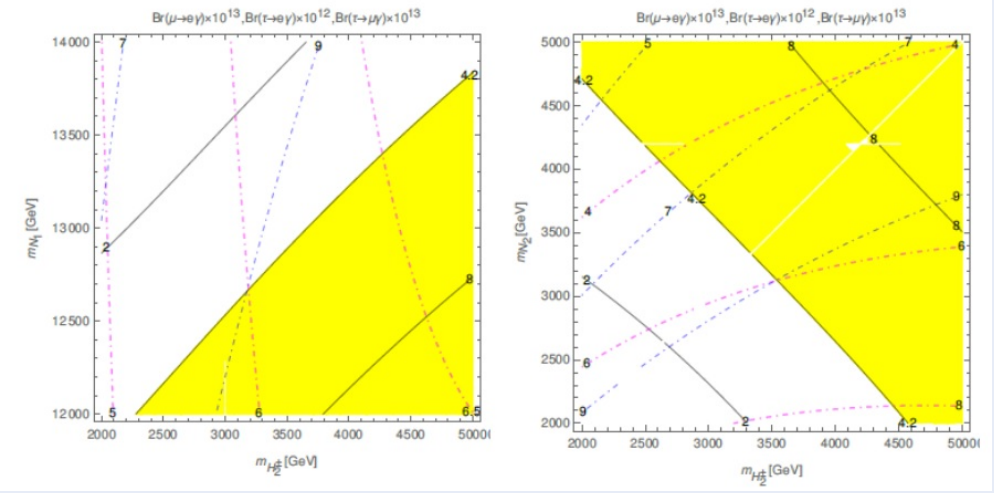

Figure 7: Contour plots of $Br\left(l_i \to l_j\gamma\right)$ dependon m_{N_1} and $m_{H_2^\pm}$ (left panel) or m_{N_2} and $m_{H_2^\pm}$ (right panel)